Indian Journal of Biochemistry & Biophysics
Vol. 57, June 2020, pp. 270-276

Fluorescence quenching and measurement of captopril in pharmaceuticals

Yahong Chen[1,2]*, Weixiao Chang[1], Xue Zhu[1,2], Ruiyong Wang[2] & Fengshou Tian[1]

[1]The Key Laboratory of Rare Earth Functional Materials and Applications, Zhoukou Normal University, Zhoukou-466 001, China
[2]College of Chemistry and Molecular Engineering, Zhengzhou University, Zhengzhou-450 001, China

Received 10 January 2018; *revised 27 November 2019*

The mechanism of fluorescence quenching of the product S in the presence of captopril was studied. The maximum emission wavelength of the product S was at 405 nm with the excitation wavelength at 316 nm. It was found that the fluorescence quenching of product S was of a static one and the binding constant (K) was 9.29 × 106 J mol^{-1}. A linear relationship was found between the relative fluorescence intensity of the product S-captopril system and the concentration of captopril. Under optimum conditions, the linear range of the calibration curve for captopril was 2~160 μg L^{-1} with a correlation coefficient of 0.9926 and a detection limit of 0.1 μg L^{-1}. The relative standard deviation (RSD) was 3.60%. The analytical results of the pharmaceuticals obtained by this novel method agreed quite well with those obtained by the KIO3 titrimetry.

Keywords: Captopril, Enzyme-catalyzed product, Fluorescence quenching

Captopril (1-[(2S)-3-mercapto-2-methylpropionyl]-L-proline) is the first orally active inhibitor of the angiotensin-converting enzyme (ACE), which is widely used in the treatment of hypertension[1] and congestive heart failure[2]. Several methods have already been reported for the quantitative determination of captopril in pharmaceutical formulations and biological fluids, including spectrophotometry[3,4], chemiluminescence[5], spectrofluorimetry[6], electrochemical detection[7,8], HPLC[9,10], and GC[11]. However, some lack of sensitivity and selectivity, others are laborious and time-consuming. In all these methods, the most common methods used are HPLC, which used to determine captopril has high sensitivity, good selectivity, and the ability of simultaneous multicomponent determination, but the sample treatment is time-consuming, require derivatization. Spectrofluorimetry is still one of the common methods used for the determination of captopril owing to its simplicity and high sensitivity.

Enzyme-catalyzed analytical kinetic methods have been extensively used for substrate, enzyme, inhibitor, and activator analysis in several areas of analytical chemistry such as in clinical, pharmaceutical, agricultural, industrial applications, and process monitorin[12]. Horseradish peroxidase (HRP; EC 1.11.1.7) is one of the most important oxidases in biology. Having the function of active molecular oxygen, HRP can enhance the transformation of H_2O_2 directly into H_2O. However, natural enzymes do have shortcomings in some aspects. For example, they are expensive and unstable in solution and have strict requirements for the experimental conditions and storage environment in order to retain their catalytic activity. Therefore, the search for a replacement for enzymes has been a significant and interesting work. The mimicking of peroxidase is one of the important trends in enzymatic analysis[13-15]. Hemin has been used as a substitute for peroxidase[16]. The complex of iron-porphyrin with β-cyclodextrin (β-CD) was proposed as a better substitute for native peroxide proteinase due to its three-dimension structure[17]. However, the catalytic activity was still much less than that of peroxidase. Hemoglobin (Hb), a necessary vehicle for oxygen carriage in the body, has the natural quaternary structure as enzymes. It contains four subunits of polypeptide and each polypeptide chain contains a heme group that may be able to serve as the active center[18-20]. In a recent paper, Hb was used to be a mimetic enzyme for HRP because they have a similar spatial structure and it is cheaper, more stable than HRP[21]. The tyrosine reacted with H_2O_2 to form the product S which was a strong fluorescence substance by the catalysis of Hb[22].

In this paper, a new, sensitive method for the determination of captopril in pharmaceuticals was

*Correspondence
E-mail: chen-yh75@163.com

established. This method was based on its fluorescence quenching to the product S with hemoglobin as the catalyst and L-tyrosine as the substrate. The fluorescence quenching mechanism was studied.

Experimental

Reagents

Hb (bovine erythrocytes) solution was prepared by dissolving a certain amount of Hb (Shanghai Boao Institute of Biochemistry, Shanghai, China) in distilled water and stored below 4°C. L-tyrosine (Beijing Chemical Plant, Beijing, China) stock solution was prepared for the concentration of 10^{-3} M. H_2O_2 solution was prepared to the concentration of 10^{-1} M. It was stored in a brown bottle in a refrigerator. Captopril (Shanghai Jianglai Institute of Biochemistry, Shanghai, China) solution was prepared to the concentration of 1.0 g L^{-1}. The working solution was diluted appropriately before use with distilled water daily. Tris-HCl buffer solutions of different pH were used throughout the present study. Doubly distilled water was used throughout. All other chemicals were of analytical-reagent grade.

The measurements of fluorescence lifetime were carried out on an FLS-920 (Edinburgh, U.K.). Other fluorescent measurements were carried out on an FP-750 spectrofluorimeter (JASCO). The temperature was controlled by using a TB-85 thermostat bath (Shimadzu), and the pH values were measured with a PHS-3C precision pH meter (Shanghai, China).

Procedures

Each color comparison tube was filled with 2.00 mL of pH 8.50 Tris-HCl buffer solutions, 4.00 mL of 1.0×10^{-3} M L-tyrosine, 0.50 mL of 1.0×10^{-5} M Hb, a proper amount of captopril solutions and 1.50 mL of 1.0×10^{-3} M H_2O_2, and then diluted with water to 10 mL. After being equilibrated in a thermostated water bath (25±0.2°C) for 40 min, the difference of the relative intensity (F_0/F) between the blank (F_0) and the sample (F) was measured at the selected maximum excitation wavelength of 316.0 nm and a maximum emission wavelength of 405.0 nm. Then, the value of F_0/F was calculated.

Results and Discussion

Spectral characteristics

The Hb-catalyzed reaction (Scheme 1) is shown below.

According to the experimental procedure, the excitation and emission spectra of product S in the absence and the presence of captopril were recorded. As shown in (Fig. 1), the excitation and emission wavelength of product S were 316 nm and 405 nm, respectively. The fluorescence strength of product S decreased in the presence of captopril, which showed that the fluorescence quenching occurred in the process.

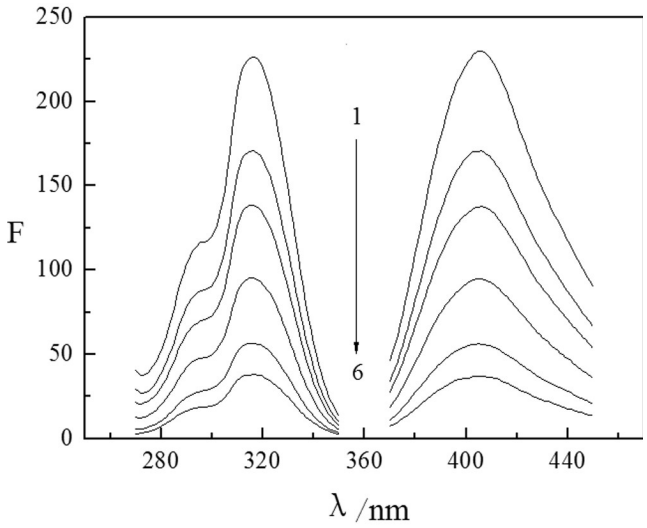

Fig. 1 — Excitation and emission spectra of product S. 1-6. Excitation spectra and emission spectra in the presence of captopril. Concentration of captopril: 0, 20, 40, 80, 120, 160 μg L^{-1}

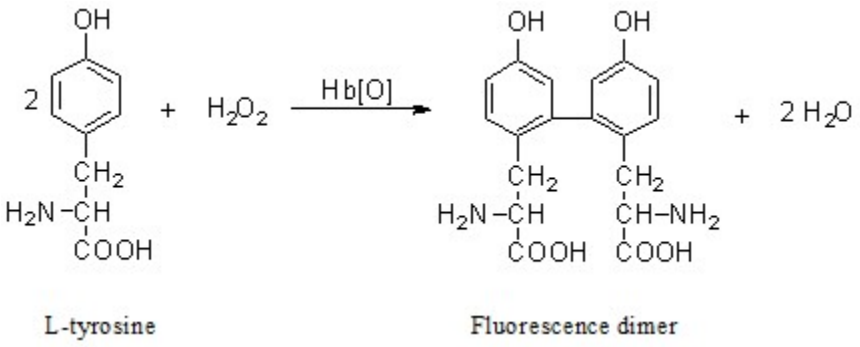

Scheme 1 — Reaction of producing fluorescence dimer

Fluorescence quenching mechanism

Generally, several mechanisms can describe the nature of fluorescence quenching, such as dynamic quenching, static quenching, combined static, and dynamic quenching. In the case of the combined static and dynamic quenching, the Stern-Volmer plot is characterized by a non-linear behavior with an upward curvature. The polynomial equation is as follows[23].

$$F_0 / F = 1 + (K_D + K_S)\,[Q] + K_D K_S\,[Q]^2 \quad \ldots (1)$$

where K_D and K_S are the dynamic and static quenching constants, respectively. F_0 and F are the fluorescence intensities in the absence and the presence of quencher. [Q] is the molar concentration of the quencher. The captopril was used as a quencher in this experiment. The Stern-Volmer equation was:

$$F_0/F = 0.7332 + 0.0308C$$

(F_0 and F are the fluorescence intensities in the absence and the presence of captopril and C was the concentration of captopril) with the coefficient 0.9929. The result in (Fig. 2) indicated that the quenching mechanism between captopril and product S was not the combined static and dynamic quenching because the Stern-Volmer plot was linear.

The dynamic quenching can be expected by the classical Stern-Volmer relationship:

$$F_0 / F = 1 + k_q \tau_0\,[Q] = 1 + k_{sv}\,[Q] \quad \ldots (2)$$

where k_q is the bimolecular quenching rate constant in L/mol s, τ_0 is the lifetime of the fluorophore in the absence of quencher, k_{SV} is the Stern-Volmer quenching constant in L mol^{-1}. In this case, a linear plot of F_0 /F vs [Q] will be obtained.

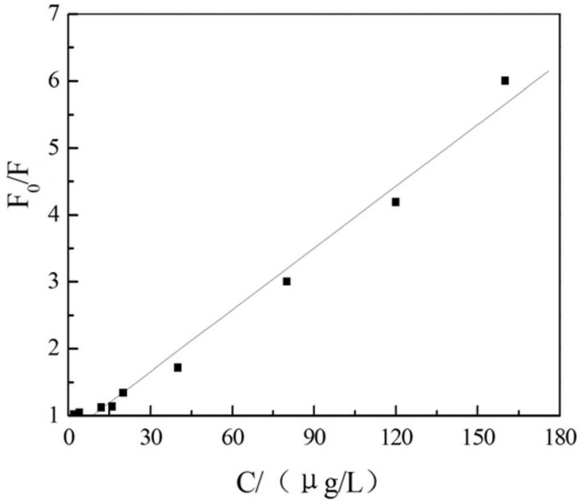

Fig. 2 — Stern-Volmer plot

In the case of static quenching, the Stern-Volmer equation is observed, giving a decrease of fluorescence intensity due to the formation of a non-fluorescent complex.

$$F_0 / F = 1 + K\,[Q] \quad \ldots (3)$$

where K is the formation constant, the Stern-Volmer plot is linear too.

The measurement of fluorescence lifetime can confirm a dynamic or static quenching process. The lifetime (τ_0) of fluorescence molecule on the excited state has no change in the presence of quencher if static quenching takes place. Reversely, τ_0 has to be shorter if dynamic quenching occurs. That is, τ_0/τ_1 =1 (τ_0 andτ_1 are the fluorescence lifetimes of fluorescence molecule in the absence and the presence of quencher) for static quenching; τ_0/τ_1= F_0 /F for dynamic quenching[24]. The fluorescence lifetimes of product S in the absence and the presence of captopril, τ_0 andτ_1 were 4.42 ns and 4.41 ns, respectively. As shown in (Fig. 3), $\tau_0/\tau_1 \cong$ 1, therefore, we suggested

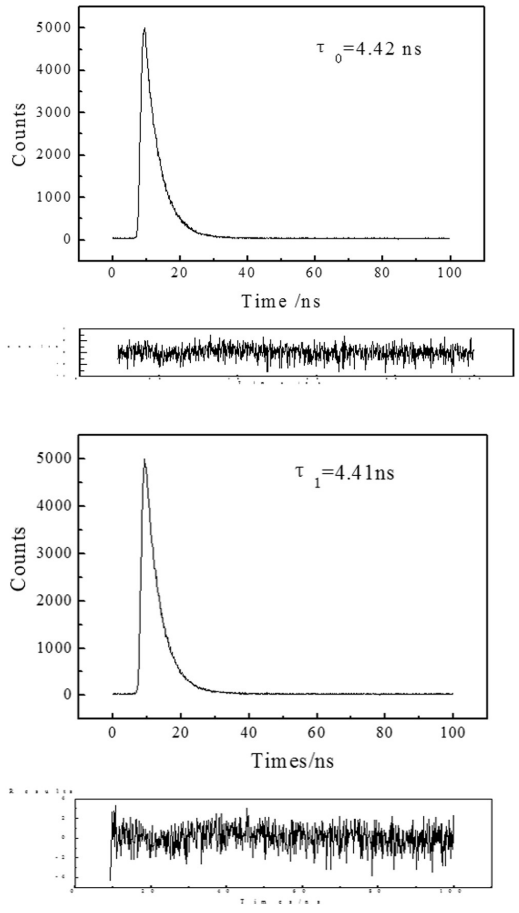

Fig. 3— The fluorescence lifetime of product S in the presence of captopril

that a static quenching process was occurring between captopril and product S.

The formation constant of static quenching

For the static quenching interaction, if there are some similar and independent binding numbers in the fluorescence molecule, the following formula can be concluded between the fluorescence molecule and quencher[25]:

$$n\mathrm{Q} + B \rightarrow Q_n\text{-B} \quad \ldots (4)$$

where B is the fluorescence molecule, Q is the quenchable molecule, Q_n-$B$is the non-fluorescence molecule, K_a is the formation constant of the reaction.

$$\mathrm{K_a} = \frac{Q_n\text{-B}}{[Q]^n[B]} \quad \ldots (5)$$

$[B_0]$ is the total concentration of fluorescence molecule (unbound and bound with the quenchable molecule), therefore, $[B_0] = [{}^{Q_n}\text{-}B] + [B]$, here $[B_0]$ is the concentration of unbound fluorescent molecule. The relationship between fluorescence intensity and the concentration of the quenchable medicament molecule is $[B]/[B_0] = F / F_0$, so there is the following equation:

$$\lg\frac{F_0 - F}{F} = \lg K + n\lg[Q] \quad \ldots (6)$$

where K is the formation constant. From Equation (6), n was the slope, and lgK was the intercept. In our research, as shown in (Fig. 4), the formation constant, K=9.29 × 10^6 L/mol, and the number of binding sites n=1.09, were obtained. The correlation coefficient of Eq. (6) was 0.9919.

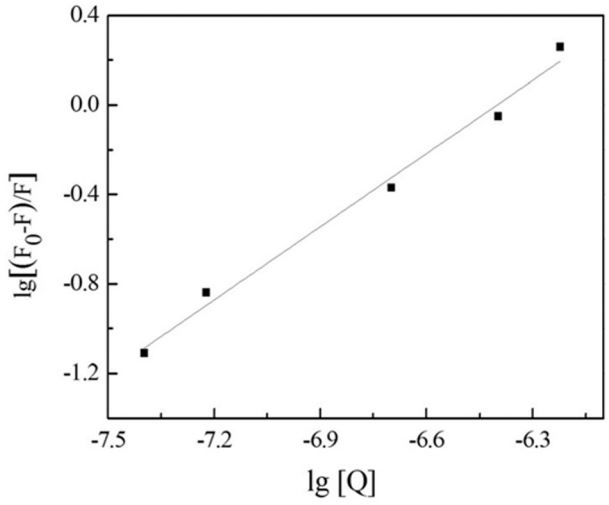

Fig. 4—lg [(F_0-F)/F] *vs* lg[Q]

The experiment results showed that the number of binding sites was n=1.09. We presumed that the carboxyl of product S bound with the sulfhydryl of captopril[26,27]. The reaction mechanism was shown in (Fig. 5).

Thermodynamic parameters

The thermodynamic parameters, Gibbs free energy change (ΔG), enthalpy change (ΔH), and entropy change (ΔS) of the reaction were obtained. ΔH and ΔS were calculated from the slope and intercept of the van't Hoff equation $\ln K = -\Delta H/RT + \Delta S/R$. ΔG were obtained according to the equation $\Delta G = \Delta H - T\Delta S$. The results were shown in (Fig. 6 & Table 1).

ΔH<0, ΔG<0 showed that the reaction was spontaneous and exothermic. What is more, both ΔH

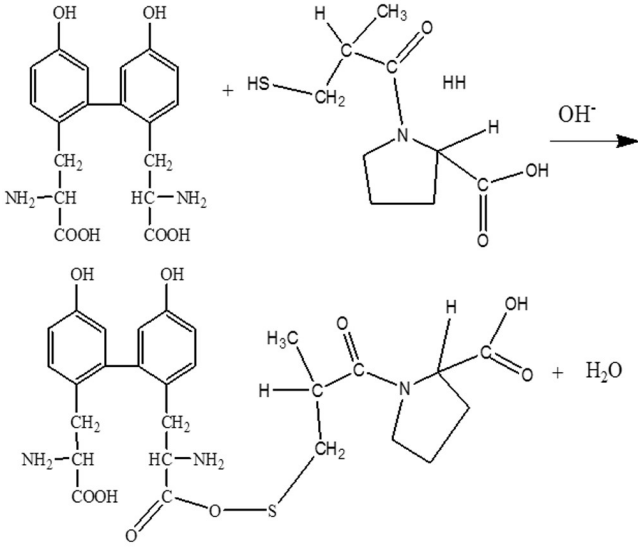

Fig. 5— The reaction mechanism

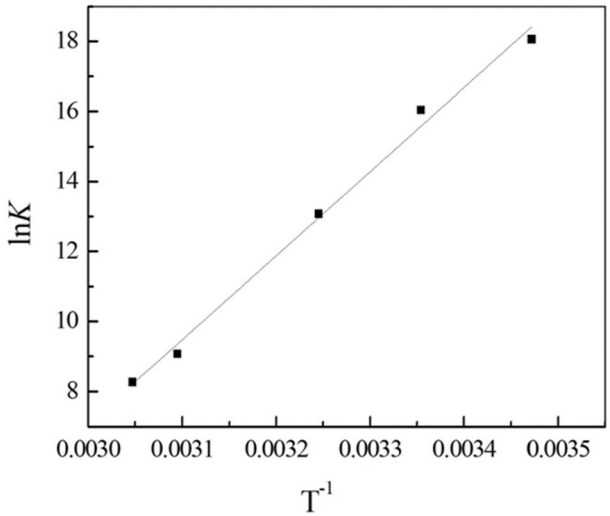

Fig. 6— ln$K$*vs*T^{-1}

Table 1 — Thermodynamic parameters

T(K)	288	298	308	323	328
K (J/mol)	6.94×107	9.29×106	4.76×105	8.69×103	3.88×103
ΔG (KJ/mol)	−43.23	−39.54	−33.48	−24.36	−22.54
ΔH (KJ/mol)		−199.70			
ΔS (J/K mol)		−540.31			

Table 2 — Optimization study for captopril determination by fluorescence quenching reaction

Variable	Range studied	Recommended value
pH	7.80-8.80	8.50
Hb (M)	$(2.00\text{-}8.00)\times10^{-7}$	5.00×10^{-7}
H_2O_2 (M)	$(0.70\text{-}2.20)\times10^{-4}$	1.50×10^{-4}
L-tyrosine (M)	$(1.00\text{-}3.50)\times/10^{-4}$	4.00×10^{-4}
Temperature (°C)	10-50	25
Time (min)	10-100	40

and ΔS were negative values indicated that van der Waals interaction and hydrogen bonds were the predominant intermolecular forces between product S and captopril[28].

The optimization of variables

The variable and ranges studied, and their optimum values, are summarized in (Table 2).

It is noted that captopril has less effect in an assay involving higher concentrations of Hb. The F_0/F increased with an increase in Hb concentration at first but decreased above 5.00×10^{-7} M. It might be due to the loss of substrate inhibition, which occurs at high Hb concentration, which could be due to the inability of captopril to promote conformational changes when Hb is at high concentration. So, 5.00×10^{-7} M of Hb was selected for further work.

The effect of H_2O_2 concentration on inhibition was studied. The F_0/F increased with the increase in H_2O_2 up to 1.50×10^{-4} M, above which it had a little effect. Thus, 1.50×10^{-4} M H_2O_2 was selected for further study. The F_0/F was greatest at pH 8.50. Considering the fluorescence intensity getting too weak at very low L-tyrosine concentration, 4.00×10^{-4} ML-tyrosine was chosen for further study.

The effect of temperature on the system was investigated in a range from room up to 50°C. The time needed to reach equilibrium, 40 min, was prolonged with the decreasing temperature. Due to the decomposition of H_2O_2 at high temperature, the temperature was kept at 25°C and the measurements were carried out after 40 min.

Table 3 — The effect of various species on hemoglobin catalyzed reaction

Species	Concentration (mg L^{-1})	F_0/F	Species	Concentration (mg L^{-1})	F_0/F
NO_3^-	40	1.89	CO_3^{2-}	20	1.83
Na^+	40	1.78	Al^{3+}	4	1.85
K^+	40	1.88	Ca^{2+}	4	1.74
NH_4^+	40	1.93	Ba^{2+}	4	1.83
F^-	40	1.86	Mg^{2+}	4	1.82
Cl^-	40	1.86	Cu^{2+}	0.2	1.82
Mn^{2+}	20	1.84	Fe^{3+}	0.2	1.81
BrO_3^-	20	1.87			

Analytical characteristics

From the results obtained under the recommended conditions (Table 2), it was found that the F_0/F of captopril on the Hb-catalyzed reaction was linear in the range 2~160 μg L^{-1}. The linear response can be fitted to an equation as follows

$$F_0/F = 0.7332 + 0.0308C$$

($r = 0.9926$, $n = 9$)

"C" is the concentration of captopril in μg L^{-1}. "r" and "n" is the linear correlation coefficient and the number of experiments, respectively. The detection limit, calculated according to the $3S_b/k$ criterion (in which "k" is the slope over the range of linear used and "S_b" is the standard deviation (n=11) of the signal from the blank), was found to be 0.1 μg L^{-1}. The relative standard deviation for 11 replicate determination of 40 μg L^{-1}captopril was 3.60%.

Interference study

Several possible inorganic ions were investigated for their interference in the determination of 40 μg L^{-1} captopril. When the permitted relative deviation is larger than ± 5.0%, the examined species may cause an alteration in the results (Table 3). It can be seen that the proposed method has good selectivity.

Applications

The current method was applied to determine the captopril in pharmaceutical preparations. Fifty tablets containing captopril were accurately weighed. An accurately weighed potion of the homogenized powder corresponding to 0.30 g of captopril was shaken for 30 min with 100 mL of the water, and the solution was filtered. Working solutions were made by appropriate dilution of concentrated sample solution with Tris-HCl buffer, so that the final concentration was in the working range for further

Table 4 — Determination of captopril in pharmaceuticals

Samples	Proposed methods[a] (mg/tablet)	KIO_3 method (mg/tablet)	t[b]
1	12.4±0.2	12.5±0.1	2.47
2	24.9±0.2	25.9±0.1	2.26

[a]Mean ± standard deviation of five determination. [t]heoretical value is 2.78, n=5, with 95% confidence level.

sample analysis. The results of the determination are listed in (Table 4). In order to examine these results, the KIO_3 method was also used for the determination by following closely the procedure described in literature[29]. The results obtained by the two different methods are statistically compared in (Table 4). It can be seen that no significant differences were found between them. This confirms the validity of the method proposed in this work.

Conclusion

The fluorescence quenching mechanism between captopril and the product S was studied. The reaction, was the static quenching process. The data of ΔH and ΔS indicated that van der Waals interaction and hydrogen bonding played a major role in the binding of captopril to product S. In addition, the binding constant, the number of binding sites and the reaction mechanism were obtained. A new spectrofluorimetric method for trace amount of captopril determination was developed based on the fluorescence quenching. The proposed method is very simple, sensitive and the detection limit was 0.1 μg L^{-1}. The method can be used for the determination of captopril in pharmaceuticals with satisfactory results.

Conflict of interest

All authors declare no conflict of interest.

Acknowledgment

Authors thank National Natural Science Foundation of China (No. 21701203) for funding.

References

1 Nagappa AN, Patil RT, Pandi V & Ziauddin K, Role of liquid membrane phenomenon in biological actions of ACE inhibitors, captopril and lisinopril. *Indian J Biochem Biophys*, 38 (2001) 412.

2 Li Y & Anand-Srivastava MB, Regulation of giα protein expression by vasoactive peptides in hypertension: molecular mechanisms. *Indian J Biochem Biophys*, 51 (2014) 467.

3 Hashemi F, Rastegarzadeh S & Pourreza N, Response surface methodology optimized dispersive liquid–liquid microextraction coupled with surface plasmon resonance of silver nanoparticles as colorimetric probe for determination of captopril. *Sensor Actuat B-Chem*, 256 (2018) 251.

4 Ravazzi CG, Franco MOK, Vieira MCR & Suarez WT, Smartphone application for captopril determination in dosage forms and synthetic urine employing digital imaging. *Talanta*, 1891 (2018) 339.

5 Fu ZF, Huang WT, Li GK & Hu YF, A chemiluminescence reagent free method for the determination of captopril in medicine and urine samples by using trivalent silver. *J Pharm Anal*, 7 (2017) 252.

6 Shi Y, Peng J, Meng XY, Huang T, Zhang JY & He Y, Turn-on fluorescent detection of captopril in urine samples based on hydrophilic hydroxypropyl-cyclodextrin polymer. *Anal Bioanal Chem*, 410 (2018) 7373.

7 Akhond G, Karimi M & Absalan R, Ramezani G & Amir M, Simultaneous determination of captopril and hydrochlorothiazide by using a carbon ionic liquid electrode modified with copper hydroxide nanoparticles. *Mikrochim Acta*, 185 (2018) 971.

8 Zarezadeh A, Rajabi HR, Sheydaei O & Khajehsharifi H, Application of a nano-structured molecularly imprinted polymer as an efficient modifier for the design of captopril drug selective sensor: Mechanism study and quantitative determination. *Mat Sci Eng C-Mater*, 94 (2019) 879.

9 Marianne AM, Simultaneous ultra performance liquid chromatography/tandem mass spectrometry determination of four antihypertensive drugs in human plasma using hydrophilic-lipophilic balanced reversed-phase sorbents sample preparation protocol. *Biomed Chromatogr*, 32 (2018) e4362.

10 Sun YH, Zhang ZJ & Zhang XF, Determination of captopril by high-performance liquid chromatography with direct electrogenerated chemiluminescence. *Spectrochim Acta Part A*, 105 (2013) 171.

11 Gatti R & Morigi R, 1,4-Anthraquinone: A new useful pre-column reagent for the determination of N-acetylcysteine and captopril in pharmaceuticals by high performance liquid chromatography. *J Pharm Biomed Anal*, 1435 (2017) 299.

12 Karthik L, Manohar R, Elamparithi K & Gunasekaran K, Purification, Characterization and Functional Analysis of a Serine Protease Inhibitor from the Pulps of *Cicer arietinum* L. (Chick Pea). *Indian J Biochem Biophys*, 56 (2019) 117.

13 Wang Y, Xu LJ & Xie W, Rapid and sensitive colorimetric sensor for H_2O_2 and Hg^{2+} detection based on homogeneous iodide with high peroxidase-mimicking activity. *Microchem J*, 147 (2019) 75.

14 Darabdhara G, Bordoloi J, Manna P & Das MR, Biocompatible bimetallic Au-Ni doped graphitic carbon nitride sheets: A novel peroxidase-mimicking artificial enzyme for rapid and highly sensitive colorimetric detection of glucose. *Sensors Actuat B-Chem*, 28515 (2019) 277.

15 Cheng XW, Huang L, Yang XY, Elzatahry AA & Deng YH, Rational design of a stable peroxidase mimic for colorimetric detection of H_2O_2 and glucose: A synergistic CeO2/Zeolite Y nanocomposite. *J Colloid Interf Sci*, 5351 (2019) 425.

16 Chaibakhsh N & Zeinab MS, Enzyme mimetic activities of spinel substituted nanoferrites (MFe2O4): A review of synthesis, mechanism and potential applications. *Mat Sci Eng C-Mater*, 99 (2019) 1424.

17 Cui C, Wang QB, Liu QY, Deng X & Zhang XM, Porphyrin-based porous organic framework: An efficient and stable peroxidase-mimicking nanozyme for detection of H2O2 and

evaluation of antioxidant. *Sensors Actuat B-Chem*, 27720 (2018) 86.

18 Wang N, Han XX, Li JY, Wang Y, Song CJ, Wang RY & Chang JB, Influence of the methyl position on the binding of 5-epi-taiwaniaquinone G to HHb investigated by spectrofluorimetry and molecular modeling. *Phys Chem Liq*, 57 (2019) 516.

19 Wang RY, Wu J, Wang LJ, Wang R & Dou HJ, Spectrofluorimetric determination of iron II based on the fluorescence quenching of cadmium/tellurium quantum dots. *Spectrosc Lett*, 47 (2014) 439.

20 Hua XY, Yang ZC, Wang ZF, Xie XX & Huang HW, Rapid modification of hemoglobin heme to form enhanced peroxidase-like activity for colorimetric assay. *Biosens Bioelectron*, 41 (2020) 100041.

21 Sun Y, Li SY, Yang YF, Feng XW & Zhang ZG, Fabrication of a thermal responsive hemoglobin (Hb) biosensor *via* Hb-catalyzed eATRP on the surface of ZnO nanoflowers. *J Electroanal Chem*, 848 (2019) 113346.

22 Chen YH, Wang QZ, Liu L & Tian FS, Fluorescence quenching and measurement of glutathione in fresh vegetables, *J Food Meas Charact*, 12 (2018) 221.

23 Kim MJ, Moon JY & Kim HS, Phosphorylation of α-syntrophin is responsible for its subcellular localization and interaction with dystrophin in muscle cells. *Indian J Biochem Biophys*, 57 (2020) 79.

24 Han XX, Wang N, Li JY, Wang Y, Wang RY & Chang JB, Identification of nafamostat mesilate as an inhibitor of the fat mass and obesity-associated protein (FTO) demethylase activity. *Chem-Biol Interact*, 297 (2019) 80.

25 Wang N, Han XX, Li JY, Wang Y, Yu WQ, Wang RY & Chang JB, Comparative study of the bindings between 3-phenyl-1H-indazole and five proteins by isothermal titration calorimetry, spectroscopy and docking methods. *J Biomol Struct Dyn*, 37 (2019) 4580.

26 Xu WL, Organic Chemistry (Beijing: Science Press), 2016.

27 Zhang M, Lv QL, Yue NN & Wang HY, Study of fluorescence quenching mechanism between quercetin and tyrosine-H_2O_2-enzyme catalyzed product. *Spectrochim Acta Part A*, 72 (2009) 572.

28 Wang ZC, Wang N, Han XX, Wang RY & Chang JB, Interaction of two flavonols with fat mass and obesity-associated protein investigated by fluorescence quenching and molecular docking. *J Biomol Struct Dyn*, 36 (2018) 3388.

29 Editorial Committee of the Pharmacopoeia of Peoples Republic of China, *The Pharmacopoeia of Peoples Republic of China (II),* (Chemical Industry Press, Beijing) 2015, 224.